Progress In Electromagnetics Research B, Vol. 56, 289–308, 2013

ANALYSIS OF NONLINEAR FRACTAL OPTICAL ANTENNA ARRAYS — A CONCEPTUAL APPROACH

Mounissamy Levy[1, 2, *], Dhamodharan Sriram Kumar[1], and Anh Dinh[2]

[1]National Institute of Technology, Tiruchirappalli 620015, India

[2]University of Saskatchewan, Saskatoon, SK S7N 5A9, Canada

Abstract—Fractal antennas have undergone dramatic changes since they were first considered for wireless systems. Numerous advancements are developed both in the area of fractal shaped elements and fractal antenna array technology for fractal electrodynamics. This paper makes an attempt of applying the concept of fractal antenna array technology in the RF regime to optical antenna array technology in the optical regime using nonlinear array concepts. The paper further discusses on the enhancement of nonlinear array characteristics of fractal optical antenna arrays using nonlinearities in coupled antennas and arrays in a conceptual manner.

1. INTRODUCTION

Nonlinear Antennas were extremely complicated in analysis, design and expensive [1]. In the 1980's and 1990's, however, came the development of antenna and antenna array concepts for commercial systems, and increases in digital signal processing complexity that pushed single antenna wireless systems close to their theoretical (Shannon) capacity. Nonlinear antennas are now seen as one of the key concept to further, many-fold, increase in both the link capacity, through pattern tailoring, spatial multiplexing, and system capacity, through interference suppression and beam forming, as well as increasing coverage and robustness for antenna designs. Furthermore, decreases in integrated circuit cost and antenna advancements have made these antennas attractive in terms of both cost and implementation even on small devices. Therefore an exponential growth have been seen in nonlinear antenna research, the inclusion

Received 26 September 2013, Accepted 6 November 2013, Scheduled 8 November 2013

* Corresponding author: Mounissamy Levy (levy_young@yahoo.com).

of nonlinear antenna technology into wireless standards, and the beginnings of widespread deployment of nonlinear antennas in wireless networks. The concept of nonlinear antennas can be extended to the optical regime for Free Space Optics (FSO) also. Section 2 discusses on the fractal theory, Section 3 discusses on the fractal optical antenna arrays and its importance. Section 4 discusses on the Iterated function systems. Section 5 discusses on the nonlinear fractal optical antenna array and finally Section 6 concludes the paper.

2. FRACTAL THEORY

Fractal theory is an emerging theory which revolutionized the way the scientists think about the nature of the world [2–10]. Derived from the Latin word meaning break apart the term fractal was originally coined by Mandelbrot to describe a family of complex shapes that possess an inherent self-similarity or self-affinity in their geometrical structure. A fractal is a recursively generated object having a fractional dimension. These intricate iterative geometrical oddities first troubled the minds of mathematicians around the turn of the twentieth century, where fractals were used to visualize the concept of the limit in calculus. What particularly confounded the mathematicians is that when they carry the limit to infinite, properties of these objects such as arc length would also go to infinity, yet the object would be bounded by a given area. However it was only during the mid-1970s that a classification was assigned to these objects and the full significance of fractal theory began to come to light. Fractal objects appear over and over throughout nature and are the product of simple stochastic mechanisms at work in the natural world. Fractal patterns often represent the most efficient solutions to achieving a goal whether it is draining water from a basin or delivering blood throughout the human body. These objects have also been used to describe the structures of fern and trees, the erosion of mountains and coastlines, and the clustering of stars in a galaxy. For these reasons it is desirable to utilize the power of fractal geometry to describe the layout of antenna arrays in the RF regime and optical antennas in the optical regime. Fractal arrays are used to increase the bandwidth of the antenna and to reduce grating lobes. These arrays have fractional dimensions that are found from generating sub array used to recursively create the fractal array. Repetitive application of a generating sub array can form a rich class of fractal array. A generating sub array is a small array at scale one ($P = 1$) where P is the scale factor, and is used to construct larger arrays of higher scales ($P > 1$). The generating sub array elements are turned on and off in a particular pattern in many cases.

A set formula for copying, scaling, and translation of the generating sub array is then followed in order to produce the fractal array. Hence, fractal arrays that are created in this manner will compose of a sequence of self-similar sub arrays. In other words, this may be conveniently considered as an array of arrays. Some recent research on Sierpinski carpet arrays, multiband arrays, fractal ultra-wideband arrays, super wideband antennas gives promising and excellent results for the application of fractal concept in antenna arrays [11–16]. The different types of fractal antenna arrays include cantor recipe set for linear fractal antenna array, planar Sierpinski carpet array, triangular, square and hexagonal antenna arrays.

3. FRACTAL OPTICAL ANTENNA ARRAYS

The absorption or emission of a photon by an electronic transition, e.g., in an atom, molecule, QD or color center is determined by the light matter interaction in the optical regime [17]. Their absorption and emission rate are limited by the weak and Omni directional interaction with light, since they are far less than the operating optical wavelength of light. Radiation in the RF regime also faced similar problems. However, these problems were encountered and addressed long ago. Since electrical circuits are much smaller than the operating wavelength usually around 50 to 60 Hz, they radiate very little. This problem of antenna length for wireless communication was addressed by introduction of various modulation schemes for analog and digital communication. To enable wireless communication they are connected to antennas that have dimensions in the order of the wavelength. These antennas are designed to effectively convert electrical signals into radiation and vice versa. Exactly the same concept can be applied in optics. By near field coupling of light into the LSPR modes of a metal NP, the interaction of quantum emitter with light can be improved to a great extent. A strong local field at the NP is formed by the LSPRs of a metal NP. If an emitter is placed in this field, its absorption and emission of radiation are enhanced. The function of the NP is then analogous to an optical antenna as in the case of an RF antenna in the RF regime. In this way excitation and emission rates can be increased and the angular, polarization and spectral dependence controlled.

The fractal antenna array concept in the RF regime requires an antenna array combined with fractal array processing technology such as Iterated Function Systems (IFS). Similarly for fractal optical antenna arrays, for incorporating the fractal concept into the optical antenna an Optical Signal Processor (OSP) combined with optical antenna arrays needed. Antenna arrays are used in the design of

apertures for modern radar and high performance communication systems in the RF regime. There are many advantages by using arrays especially their high gain, directivity, and the possibility of beam steering which is called beam scanning. Arrays can be mainly classified into two types based on their dimension, single dimensional array and multidimensional array. The multidimensional array consists of two dimensional arrays or planar array and three dimensional arrays. Depending on the Lattice structure arrays are classified as uniform and non-uniform arrays. Non uniform linear arrays are called as nonlinear arrays. Uniform arrays are called as periodic arrays. Depending upon the distribution of array elements the arrays can be classified into dense arrays and sparse arrays. Table 1 shows the trade-offs between dense and sparse antenna arrays for various properties [18]. Much of the explanation about antenna array is available in the texts [19–23].

Table 1. Trade-offs between dense and sparse antenna arrays.

Property	Dense array		Sparse array
Variance of the antenna match	High		Low
Average side lobe levels	Low		Moderate
Peak side lobe levels	Moderate		Low
Hardware density	High		Low
Power per element	Low		High
Aperture size needed	Small		Large
Number of elements for an aperture	Many		Few
Coupling	Strong		Weak
Achievable Bandwidth	$> 10:1$		$\gg 10:1$

4. ITERATED FUNCTION SYSTEMS (IFS)

For the construction of a broad spectrum of fractal geometries, Iterated Function Systems (IFS) are powerful mathematical toolsets [18]. These IFS are constructed from a finite set of contraction mappings, each based on an affine linear transformation performed in the Euclidean plane. The most general representation of an affine linear transformation ω_n consists of six real parameters (a_n, b_n, c_n, d_n, e_n, f_n) and is defined as

$$\begin{pmatrix} x' \\ y' \end{pmatrix} = \omega_n \begin{pmatrix} x \\ y \end{pmatrix} = \begin{pmatrix} a_n & b_n \\ c_n & d_n \end{pmatrix} \begin{pmatrix} x \\ y \end{pmatrix} + \begin{pmatrix} e_n \\ f_n \end{pmatrix} \tag{1}$$

$$w_n(x, y) = (a_n x + b_n y + e_n, c_n x + d_n y + f_n) \tag{2}$$

The parameters of the IFS are often expressed using the compact notation

$$\left(\begin{array}{cc||c} a_n & b_n & e_n \\ c_n & d_n & f_n \end{array}\right) \tag{3}$$

where coordinates x and y represent a point belonging to an initial object and coordinates x' and y' represent a point belonging to the transformed object. To scale rotate, shear, reflect and translate any arbitrary object, this general transformation can be used. The parameters a_n, b_n, c_n and d_n control rotation and scaling while e_n and f_n control linear translation. Consider a set of N affine linear transformations $\omega_1, \omega_2, \omega_3, \omega_4, \ldots, \omega_N$. This set of transformations forms an IFS that can be used to construct a fractal of stage $\ell+1$ from a fractal of stage ℓ

$$F_{\ell+1} = W(F_\ell) = \cup_{n=1}^{N} w_n(F_\ell) \tag{4}$$

where W is the Hutchinson operator and F_ℓ is the Fractal of stage ℓ. The pattern produced by the Hutchinson operator is referred to as the generator of the fractal structure. If each transformation reduces the size of the previous object, then the Hutchinson operator can be applied an infinite number of times to generate the final fractal geometry, F_∞. For example, if set F_0 represents the initial geometry, then this iterative process would yield a sequence of Hutchinson operators that converge upon the final fractal geometry F_∞.

$$F_1{=}W(F_0)\,,\ F_2{=}W(F_1)\,,\ \ldots,\ F_{k+1}{=}W(F_k)\,,\ \ldots,\ F_\infty{=}W(F_\infty) \tag{5}$$

If the IFS is truncated at a finite number of stages L, then the object generated is said to be a prefractal image, which is often described as a fractal of stage L.

The IFS approach is the most common method used to construct deterministic fractal array geometries; however, deterministic fractals may not resemble natural objects very closely because of their perfect symmetry and order. But random fractals more closely resemble natural objects because their objects are often created using purely stochastic means on the other hand. However these objects are difficult to work with especially in the context of optimization, because their structures cannot be recreated with exact precision. A specialized type of fractal geometry called a fractal random tree was developed in an effort to bridge the gap between deterministic and random fractals. This new construct combines together properties of both deterministic and random fractal geometries. Therefore a more generalized expansion of deterministic fractal based geometry is introduced, called polyfractal geometry. In order to construct a poly fractal the IFS technique introduced must be expanded to handle

multiple generators. Polyfratcal arrays are constructed from multiple generators, $1, 2, \ldots, M$, each of which is having a corresponding Hutchinson operator $W_1, W_2, W_3, \ldots, W_M$. Each Hutchinson operator W_m in turn contains N_m affine linear transformations, $\omega_{m,1}, \omega_{m,2}, \omega_{m,3}, \ldots, \omega_{m,Nm}$. The IFS code for generating an inverted Sierpinski gasket and the IFS code and associated connection factors for Sierpinski based polyfractal geometries are shown in Table 2 and Table 3 respectively. The same concept can be applied to optical antenna arrays to get the novel smart optical antenna arrays using smart-fractal concepts. A fractal optical antenna can be designed using the application of fractal concept properly incorporated into an optical antenna.

Table 2. IFS code for generating an inverted Sierpinski gasket.

w	a	b	c	d	e	f
1	1/2	0	0	1/2	0	$\sqrt{3}/4$
2	1/2	0	0	1/2	1/2	$\sqrt{3}/4$
3	1/2	0	0	1/2	1/4	0

Table 3. IFS code and associated connection factors for Sierpinski-based polyfractal geometries.

	w	a	b	c	d	e	f	$: \kappa$
Generator 1	1	1/2	0	0	1/2	0	$\sqrt{3}/4$	: 1
	2	1/2	0	0	1/2	1/2	$\sqrt{3}/4$	: 1
	3	1/2	0	0	1/2	1/4	0	: 2
Generator 2	1	1/2	0	0	1/2	0	$\sqrt{3}/4$	: 2
	2	1/2	0	0	1/2	1/2	$\sqrt{3}/4$	: 1
	3	1/2	0	0	1/2	1/4	0	: 2
	4	1/2	0	0	$-1/2$	1/4	$\sqrt{3}/2$	: 1

5. NONLINEAR FRACTAL CONCEPT FOR OPTICAL ANTENNA ARRAY

The concept of Nano antennas has emerged in optics as an enabling technology for controlling the spatial distribution of light on sub diffraction length scales. Analogously to classical antenna design, the objective of optical antenna design is the optimization and control of

the energy transfer between a localized source acting as a receiver or transmitter, and the free radiation field. Most of the implemented optical antenna designs operate in the linear regime that is the radiation field and the polarization fields are linearly dependent on each other. When this linear dependence breaks down, however new interesting phenomena arise, such as frequency conversion, switching and modulation. Beyond the ability of mediating between localized and propagating fields, a nonlinear optical antenna provides the additional ability to control the interaction between the two. The nonlinear antenna converts the frequency of the incident radiation centered at by a predefined amount into a new frequency band centered at. It is vital to know the basic properties of nonlinear antenna and then focus on the nonlinearities achievable either in single NP systems or more complex-coupled NP systems. In practice the use of nonlinear materials either metals or dielectrics in the design of optical antennas is a promising route towards the generation and control of optical information. Optical antennas link objects to light [17]. The main idea is shown in the block diagrams in Figure 1 and Figure 2. In the first method as shown in Figure 1, the linear optical antenna array is considered first and then the nonlinear fractal antenna concept using fractal theory is applied which results in a nonlinear fractal optical antenna array. The optical signal processor controls the optical antenna array and the nonlinear fractal part. In the Second method shown in Figure 2, the nonlinear optical antenna array is considered first and the linear fractal concept is applied using fractal theory which results in the nonlinear array. The optical signal processor controls both the part, for tailoring the beam shape and for producing the beam in the desired direction. Figures 3 to 6 show the array factor pattern and directivity pattern [7] of the fractal antenna array in the RF regime which is essentially the same for optical antenna array when operated

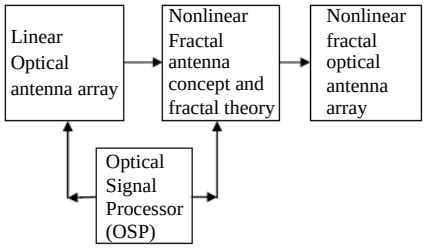

Figure 1. Block diagram of nonlinear fractal optical antenna array system, First method.

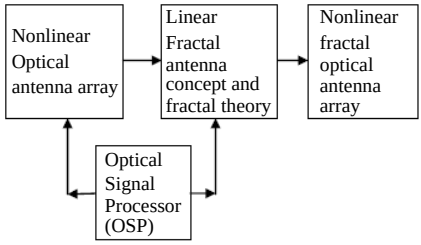

Figure 2. Block diagram of nonlinear fractal optical antenna array system, Second method.

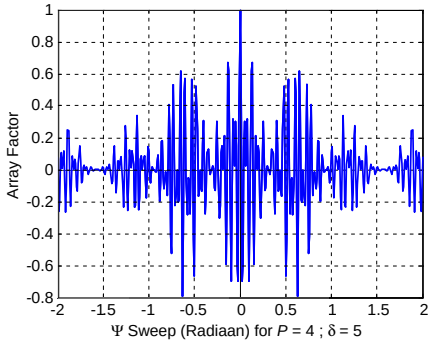

Figure 3. Fractal optical antenna array pattern for $P = 4$; $\delta = 3$ in the optical regime is the same as in RF regime when operated in fundamental mode.

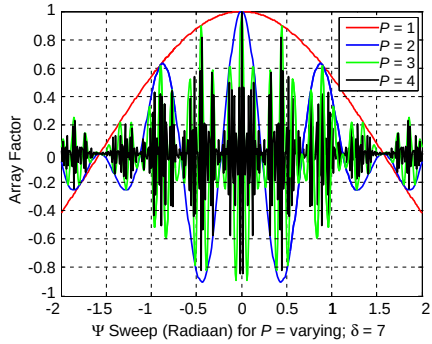

Figure 4. Fractal optical antenna array pattern for $P = 1$ to 4; $\delta = 7$ in the optical regime is the same as in RF regime in fundamental mode.

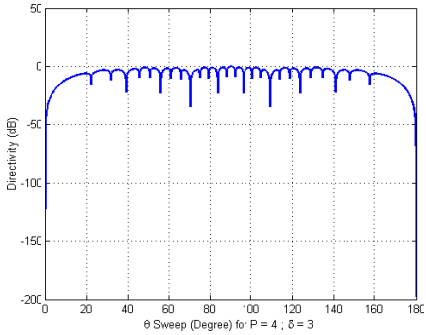

Figure 5. Fractal optical antenna array directivity pattern for $P = 4$; $\delta = 3$ in the optical regime is the same as in RF regime in fundamental mode.

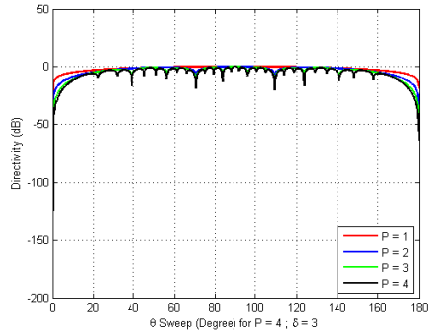

Figure 6. Fractal optical antenna array directivity pattern for $P = 1$ to 4; $\delta = 3$ in the optical regime is the same as in RF regime in fundamental mode.

in the fundamental mode of operation [17]. Consider a quantum object, such as a molecule, QD or atom. The typical timescale for an electric dipole transition to emit a photon is on the order of nanoseconds and the photon is emitted in dipole angular pattern. This slow undirected interaction places several limits on their absorption and emission of light. First, the long radiative lifetime limits the maximum amount of photons that can be emitted per second, i.e., the maximum brightness. Second, if faster competing loss channels and/or depahsing are present

as is often the case for condensed matter at room temperature; a slow interaction becomes a weak interaction. The emitter then absorbs only a small fraction of the incident light, and radiates its energy with a low efficiency. Third, the undirected nature of the interaction makes it challenging to efficiently collect the emission and further reduces the probability of absorption under illumination.

The interaction of the emitter with light can be improved by near field coupling to a second larger but still small object: an antenna. The emitter now mainly absorbs and emits light through the modes of the antenna. By suitably designing the antenna, the absorption and emission rates can be enhanced. Furthermore the angular, polarization and spectral dependence of both the emission and absorption can be controlled. Consider a number of such objects are placed near the light source in an angular split. Let there be 'n' such objects. Considering uniform distribution in space of a two dimensional medium the angular separation 'θ' between one object and the other object for linear spacing in the theta plane is given by

$$\theta = \frac{2\pi}{n} \tag{6}$$

Let us consider a simple nonlinear spacing of the objects placed at 0, nX°, n^2X°, n^3X°, ... A suitable mechanism should be devised to select a particular antenna. Optical Signal Processor (OSP)is used to select a particular object depending upon the requirement and the optical antenna will radiate in that particular direction. Depending upon the element selected the excitation ratio on the selected element to the reference element is given by [17]

$$\frac{\gamma_{exc,n}}{\gamma_{exc,0}} = \frac{|p.E_{loc}(r,\varphi,\theta,\omega)|^2}{|p \cdot E_{loc,0}(r,\varphi,\theta,\omega)|^2} \tag{7}$$

where $\gamma_{exc,n}$ is the excitation rate on the nth element and $\gamma_{exc,0}$ is the excitation rate on the reference element, p is the unit vector in the direction of the orientation of the dipole moment, $E_{loc}\,(r,\,\varphi,\,\theta,\,\omega)$ is the resulting local electric field at the emitter position on the emitter dipole moment, $E_{loc,0}\,(r,\,\varphi,\,\theta,\,\omega)$ is the resulting local electric field at the reference position on the reference dipole moment.

The power from each emitter is given by

$$P\,(r,\varphi,\theta,\omega) = \frac{|E\,(r,\varphi,\theta,\omega)|^2}{2Z_0} \tag{8}$$

where $E\,(r,\,\varphi,\,\theta,\,\omega)$ is the electric field on each emitter and $P(r)$ is given by

$$P\,(r) = \int_\pi \int_{2\pi} P\,(r,\varphi,\theta,\omega)\sin\theta d\varphi d\theta \tag{9}$$

The ratio of excitation to the nth element with respect to the reference element is given by

$$\frac{\gamma_{r.n}}{\gamma_{r,0}} = \frac{P_n(r)}{P_0(r_0)} \tag{10}$$

The coupling efficiency is given by

$$\eta_c(r) = \frac{\int_\pi \int_{2\pi} P(r, \varphi, \theta, \omega) \sin\theta d\varphi d\theta}{P(r)} \tag{11}$$

The ratio of power dissipated by the nth element to the reference element power emitted is given by

$$\frac{\gamma_{n,diss}}{\gamma_{r,0}} = \frac{P_{n,diss}}{P_0(r_0)} \tag{12}$$

$$\eta_q = \frac{\gamma_r}{\gamma_r + \gamma_{nr}} \tag{13}$$

$$\gamma_{nr} = \gamma_{diss} + \gamma_{int} \tag{14}$$

$$\gamma = \gamma_r + \gamma_{nr} \tag{15}$$

The loss in power is proportional to the square of the current and the total loss in the antenna array follows the equation

$$P_{tot} = n\left(P_{dir} + P_{feed} + P_{ref}\right) = n\left(I_{dir}^2 + I_{feed}^2 + I_{ref}^2\right) R \tag{16}$$

with n being the number of antenna elements, I_{dir}, I_{feed}, and I_{ref} being the current inside the director, feed element and reflector respectively and R being the resistance of the nano rod.

A measure of the total loss in the array is the absorption A, which can be deduced from the reflectance R, transmittance T and scattered intensity S by the simple expression

$$A = 1 - T - R - S \tag{17}$$

where scattering is negligible in the array structure. Since the reflected intensity of the antenna array depends on the direction of illumination, and transmittance is equal for the different illumination angles, the absorption depends on the angle of incidence.

For any antenna, both at RF and optical frequencies, it is very important to quantify how directed the emission is. The antenna directivity D is defined as the power emitted into desired direction compared with the power averaged over all directions. The angular directivity D describes how effectively the power is concentrated into a particular direction, a very small solid angle or approximately a plane wave. $D = 1$ for a hypothetical isotropic emitter, while the maximum of the angular directivity for an EHD in an isotropic homogeneous environment is 1.5. An even more important figure of merit for

antenna performance is the power gain, a key figure which combines directivity and efficiency. The antenna gain quantifies how much the total efficiency is increased, compared with an isotropic emitter. Thus the gain quantifies how much the antenna improves the emission by redirecting it into a given angle. When placing an antenna near an emitter, the excitation and emission rates are both altered. The enhancement of the emission rate into a certain angle and polarization is equal to the excitation rate enhancement for illumination by a plane wave under the same angle with the directivity is given by

$$D\left(\phi,\theta\right) = \frac{4\pi P(r,\phi,\theta)}{P(r)} \tag{18}$$

The antenna gain quantifies how much the total efficiency is increased, compared with an isotropic emitter with $\eta_{q,0} = 1$ and is given by

$$G\left(\phi,\theta\right) = \eta_q D\left(\phi,\theta\right) \tag{19}$$

for same polarization. Thus the changes are linked by the angular directivity D. This is the reciprocity theorem for antennas.

Hence the gain quantifies how the antenna improves the emission by redirecting it into a given angle.

The reciprocity theorem for antennas is mathematically described as

$$\frac{\gamma_{exc}(\phi,\theta)}{\gamma_{exc,0}} = \frac{D\left(\phi,\theta\right)}{D_0}\frac{\gamma_r}{\gamma_{r,0}} \tag{20}$$

in which the subscript 0 marks again the reference situation that can be freely chosen. The reciprocity assumes that the excitation and emission occur at the same wavelength and that the excitation rate is calculated for plane wave illumination with a polarization equal to the emission polarization. The equation can be adapted for arbitrary polarization and illumination.

The input impedance of the optical antenna may generally be written using the nano circuit model as

$$z_{in} = \frac{1}{1/Z_a - j\omega C} \tag{21}$$

where $C = \epsilon_0 S/g$ is the gap nano capacitance. The real and imaginary parts of the intrinsic antenna impedance $Z_a = R_a - jX_a$ may then be expressed as a function of the input resistance and reactance given by

$$R_a = \frac{R_0}{1 + \omega C\left(2X_0 + \omega C\left(R_0^2 + X_0^2\right)\right)} \tag{22}$$

$$X_a = \frac{X_0 + \omega C(R_0^2 + X_0^2)}{1 + \omega C\left(2X_0 + \omega C\left(R_0^2 + X_0^2\right)\right)} \tag{23}$$

in order to de-embed the intrinsic impedance of the optical antenna when evaluated with full-wave simulations. The input impedance of fractal antenna is given by

$$z_{in(FRACT)} = F * z_{in} \tag{24}$$

where F accounts for the fractal array impedance factor. If a NP load with arbitrary permittivity ϵ_L in the gap is included, then the input impedance is changed to

$$R_{in} = \frac{g^2 R_a}{g^2 - 2\omega\epsilon_L g S X_a + \omega^2 \epsilon_L^2 S^2 (R_a^2 + X_a^2))} \tag{25}$$

$$X_{in} = \frac{g(gX_a - S(R_a^2 + X_a^2)\omega\epsilon_L}{g^2 - 2\omega\epsilon_L g S X_a + \omega^2 \epsilon_L^2 S^2 \left(R_a^2 + X_a^2\right))} \tag{26}$$

For simplicity, complete filing of the gap by the NP is assumed. However, more complex configurations with parallel or series combination of NPs with different fractal configurations can be considered. Some fractal configurations can include the Cantor recipe set for the linear array or the Sierpinski carpet for planar array. The open-circuit resonance of interest for matching and radiation purpose is obtained when R_{in} is a maximum and $X_{in} = 0$ at the radian frequency given by

$$\omega_0 = \frac{gX_a}{S(R_a^2 + X_a^2)\epsilon_L} \tag{27}$$

which is the most celebrated parallel resonance equation between the intrinsic impedance and the load impedance. Enabling tuning of the resonance frequency by increasing the load permittivity, the operational bandwidth of the antenna also called the sensitivity s to the load permittivity is defined as

$$s = \frac{\partial\omega_0}{\partial\epsilon_L} \tag{28}$$

At the operating optical frequency, the intrinsic impedance of the nano antenna is determined by the sensitivity. The sensitivity of the optical antenna is optimized by the proper choice of the geometrical antenna parameters and the operational bandwidth for the application of interest. The fractal geometry plays a major role in this part. Linear array, planar array, triangular array, hexagonal array, concentric circular ring sub-array generators plays a vital role in determining the geometrical parameters of the optical antenna array using smart fractal concepts. This is particularly important for smart antenna, biosensing or SERS applications as the proper tailoring of the antenna intrinsic impedance is directly related to its sensitivity and bandwidth.

Nonlinear optics exploits the nonlinear relationship between the exciting electric field $\vec{E}$ and the resulting polarization $\vec{P}$ in general. The relationship between $\vec{E}$ and $\vec{P}$ is linear for weak excitation fields, and most optical antennas operate in this regime. However, for strong excitations the response $\vec{P}$ depends on higher powers of $\vec{E}$, which gives rise to interesting and technologically important phenomena, such as frequency mixing, rectification or self-phase modulation. The nonlinear relation between $\vec{P}$ and $\vec{E}$ can be expressed as a series given by

$$\vec{P} = \epsilon_0 \left[\chi^{(1)} \vec{E} + \chi^{(2)} \vec{E}\vec{E} + \chi^{(3)} \vec{E}\vec{E}\vec{E} + \chi^{(4)} \vec{E}\vec{E}\vec{E}\vec{E} + \ldots \right] \tag{29}$$

where the susceptibilities χ are tensors of rank $n+1$. The polarization $\vec{P}$ constitutes a secondary source current that, when inserted into Maxwell equations, gives rise to a set of nonlinear differential equations. Since the light matter interaction is inherently weak, however it is very usual to approximate the response of a charged NP by a driven harmonic oscillator that is Lorentz atom model. The charges oscillating at the new frequencies induce polarization currents $P(t)$, that give rise to electromagnetic radiation at those new frequencies. For the driving field $E(t) = E\cos(\omega t)$, the induced SHG nonlinear polarization is given by

$$P^2(t) = \epsilon_0 \chi^{(2)} E^2(t) = 2\epsilon_0 \chi^{(2)} E^2 + 2\epsilon_0 \chi^{(2)} E^2 \cos(2\omega t) \tag{30}$$

A constant dispersion free nonlinear susceptibility is assumed for simplicity. The THG components are given by

$$P^3(t) = \epsilon_0 \chi^{(3)} E^3(t) = \frac{1}{4}\epsilon_0 \chi^{(3)} E^3 \cos(3\omega t) + \frac{3}{4}\epsilon_0 \chi^{(3)} E^3 \cos(\omega t) \tag{31}$$

where the first term describes the THG and the second term is the Kerr nonlinearity which is the change of the refractive index of the material at the fundamental frequency. The driving field contains more than one discrete frequency, nonlinear response at mixing frequencies $\omega_1 + \omega_2$, difference $\omega_1 - \omega_2$, or four wave mixing (4WM) given by $\omega_1 \pm \omega_2 \pm \omega_3$. Another class of nonlinear process involves a sequence of distinct optical interactions, such as the absorption of two photons followed by the emission of one photon, a process referred as TPL which is a third order nonlinear process. It is a very powerful tool to study local fields near metal nano antennas because of its quadratic intensity dependence. The Poynting theorem for the average rate of energy dissipation in a polarizable metal is given by

$$P_{abs} = -\int_V \left\langle \vec{j}(\vec{r},t) \cdot \vec{E}(\vec{r},t) \right\rangle dV \tag{32}$$

where $\langle \ldots \rangle$ denotes the time average and $\vec{j} = d\vec{P}/dt$ is the polarization current density. For a time harmonic field given by $\vec{E}(\vec{r},t) = \mathrm{Re}[\vec{E}(\vec{r},\omega)\exp(-i\omega t)$, the Equation (32) changes to

$$P_{abs} = -\frac{1}{2}\int_V \mathrm{Re}\left[\vec{j}\left(\vec{r},\omega\right)\cdot\vec{E}\left(\vec{r},\omega\right)\right]dV \tag{33}$$

The lowest order term in Equation (29) contributes to the P_{abs} that is associated with $\chi^{(1)}$ and is responsible for linear absorption is given by

$$P_{abs}^{(1)} = \frac{\omega}{2}\int_V \mathrm{Im}\left[\chi^{(1)}\left(\omega\right)\right]\vec{E}\vec{E}^{*}dV \tag{34}$$

Similarly the next highest contributing term associated with $\chi^{(3)}$ and responsible for two-photon absorption is given by

$$P_{abs}^{(3)} = \frac{\omega}{2}\int_V \mathrm{Im}\left[\chi^{(3)}\left(\omega,-\omega,\omega\right)\right]\vec{E}\vec{E}^{*}\vec{E}\vec{E}^{*}dV \tag{35}$$

For an extended isotropic material irradiated by a plane wave, the above equation reduces to

$$P_{abs}^{(3)} \sim \mathrm{Im}\left[\chi^{(3)}\right]\left|\vec{E}\right|^4 \tag{36}$$

The assemblies of metal NPs play a vital role in many applications. Optical plasmonic properties depend on the interplay between its constituting NPs. However, the near field interaction of an NP with its adjacent NP results in couple LSPRs. Even though the absolute LSPR shift depends on the size, shape, type, surrounding medium, a universal rule of the fractional shift of the wave length $\Delta\lambda/\lambda_0$ can be observed when the distance S between NPs is scaled by their characteristic dimension D given by

$$\frac{\Delta\lambda}{\lambda_0} = \frac{\lambda_1-\lambda_0}{\lambda_0} \sim \kappa\exp\left(-\frac{S}{\tau D}\right) \tag{37}$$

For the coherent control of nano optical excitations, the relation between local electric field and the external incident electric field is given by

$$\vec{E}\left(\vec{r},t\right) = \int_{space} d\vec{r}' \int_{-\infty}^{t} dt' S\left(\vec{r},\vec{r}',t-t'\right)\vec{E}_{ext}\left(\vec{r}',t'\right) \tag{38}$$

For frequency domain description, the convolution leads to a simple multiplication

$$\vec{E}\left(\vec{r},\omega\right) = \tilde{\mathbf{S}}\left(\vec{r},\omega\right)\vec{E}_{ext}\left(\omega\right) \tag{39}$$

where $\tilde{\mathbf{S}}$ stands for the tensorial linear response function. The above equation can be written in component notation as a sum over two terms

$$\vec{E}(\vec{r},\omega) = \begin{pmatrix} E_x(\vec{r},\omega) \\ E_y(\vec{r},\omega) \\ E_z(\vec{r},\omega) \end{pmatrix} = \sum\nolimits_{j=1}^{2} \begin{pmatrix} S_x^j(\vec{r},\omega) \\ S_y^j(\vec{r},\omega) \\ S_z^j(\vec{r},\omega) \end{pmatrix} E_{ext}^j(\omega) \tag{40}$$

Both the external transverse frequency domain field and the local field are complex valued quantity given by

$$E_{ext}^j(\omega) = A_{ext}^j(\omega)\, e^{i\varphi_{ext}^j(\omega)} \tag{41}$$

and the Fourier inverse gives

$$\vec{E}(\vec{r},t) = F^{-1}\left\{\vec{E}(\vec{r},\omega)\right\} \tag{42}$$

and the interaction with the wave function $\boldsymbol{\psi}(r,\, t)$ of a quantum mechanical system gives

$$V(\vec{r},t) = -\mu \cdot \vec{E}(\vec{r},t) \tag{43}$$

with the dipole operator μ in electric dipole approximation. For local polarization mode interference, the far field polarization components are orthogonal to each other and the total far field intensity is given by

$$I_{ext}(\omega) \sim \left|\vec{E}_{ext}(\omega)\right|^2 = \left|A_{ext}^1(\omega)\right|^2 + \left|A_{ext}^2(\omega)\right|^2 \tag{44}$$

For the near field case the total local intensity is obtained from

$$I(\vec{r},\omega) \sim \left|\vec{E}(\vec{r},\omega)\right|^2 = \sum\nolimits_{n=x,y,z} \left|\sum_{j=1}^{2} S_n^j(\vec{r},\omega)\, A_{ext}^j(\omega)\, e^{i\varphi_{ext}^j(\omega)}\right|^2 \tag{45}$$

For local pulse compression Equations (40) and (41) can be written as

$$\vec{E}(\vec{r},\omega) = \left[\begin{pmatrix} S_x^1(\vec{r},\omega) \\ S_y^1(\vec{r},\omega) \\ S_z^1(\vec{r},\omega) \end{pmatrix} A_{ext}^1(\omega) + \begin{pmatrix} S_x^2(\vec{r},\omega) \\ S_y^2(\vec{r},\omega) \\ S_z^2(\vec{r},\omega) \end{pmatrix} A_{ext}^2(\omega)\, e^{-i\Delta\varphi_{ext}(\omega)}\right] e^{i\varphi_{ext}^1(\omega)} \tag{46}$$

where the external phase difference is defined in the frequency domain by

$$\Delta\varphi_{ext}(\omega) = \varphi_{ext}^1(\omega) - \varphi_{ext}^2(\omega) \tag{47}$$

For fixed phase difference $\Delta\varphi_{ext}(\omega)$, the local spectral phase can be changed to a modified phase

$$\varphi_x^{mod}(\vec{r},\omega) = \varphi_x(\vec{r},\omega) + \varphi_{ext}^1(\omega) \tag{48}$$

For a short pulse, $\varphi_x^{mod}(\vec{r},\omega) = 0$, therefore

$$\varphi_{ext}^{1}(\omega) = -\varphi_x(\vec{r},\omega) \tag{49}$$

For optimal control, we have to identify a suitable observable whose expectation value shall approach a given target. For controlling local fields on a spatial scale, let us start with the local spectral density defined in Equation (45) and integrate over frequency to obtain the local linear flux

$$F(\vec{r}) = \int_0^\infty d\omega \sum\nolimits_{n=x,y,z} \left| \sum\nolimits_{j=1}^{2} S_n^j(\vec{r},\omega) A_{ext}^j(\omega) e^{i\varphi_{ext}^j(\omega)} \right|^2 \sim \int_0^\infty d\omega I(\vec{r},\omega) \tag{50}$$

The objective is to enhance the local flux at an arbitrary position $\vec{r}_1$ and to suppress it at a different position $\vec{r}_2$. The fitness function is

$$f\left[\vec{E}_{ext}(\omega)\right] = F(\vec{r}_1) - F(\vec{r}_2) \tag{51}$$

A necessary condition for global optimal control is given by

$$\frac{\delta}{\delta\left[\Delta\varphi_{ext}(\omega)\right]} f\left[\vec{E}_{ext}(\omega)\right] = 0 \tag{52}$$

The solution for Equation (52) for a linear response is given by

$$\begin{aligned}&\Delta\varphi_{ext}(\omega)\\ =&\arctan\left\{\frac{S_{mix}(\vec{r}_2,\omega)\sin[\theta_{mix}(\vec{r}_2,\omega)] - S_{mix}(\vec{r}_1,\omega)\sin[\theta_{mix}(\vec{r}_1,\omega)]}{S_{mix}(\vec{r}_1,\omega)\cos[\theta_{mix}(\vec{r}_1,\omega)] - S_{mix}(\vec{r}_2,\omega)\cos[\theta_{mix}(\vec{r}_2,\omega)]}\right\} + k\pi\end{aligned} \tag{53}$$

where k is an integer. The response-function mixing amplitude with the condition $S_{mix}(\vec{r},\omega) \geq 0$ and mixing angle $\theta_{mix}(\vec{r},\omega)$ is given by

$$S_{mix}(\vec{r},\omega) e^{i\theta_{mix}(\vec{r},\omega)} = \sum\nolimits_{n=x,y,z} S_n^1(\vec{r},\omega) \left[S_n^2(\vec{r},\omega)\right]^* \tag{54}$$

The optimum external field amplitude is given by

$$A_{ext}^j(\omega) = \gamma^j(\omega)\sqrt{I_{in}(\omega)} \tag{55}$$

For optimum transmission coefficients, the solution pairs are given by

$$\left[\gamma^1(\omega), \gamma^2(\omega)\right] \in \left\{[0,0], \left[1, -\frac{C_{mix}(\omega)}{C_2(\omega)}\right], \left[-\frac{C_{mix}(\omega)}{C_1(\omega)}, 1\right], [1,1]\right\} \tag{56}$$

with the coefficients given by

$$C_j(\omega) = \sum\nolimits_{n=x,y,z} \left(\left|S_n^j(\vec{r_1},\omega)\right|^2 - \left|S_n^j(\vec{r},\omega)\right|^2 \right) \tag{57}$$

and

$$\begin{aligned}C_{mix}(\omega) = &S_{mix}(\vec{r}_1,\omega)\cos[\theta_{mix}(\vec{r}_1,\omega) + \Delta\varphi_{ext}(\omega)]\\ &- S_{mix}(\vec{r}_2,\omega)\cos[\theta_{mix}(\vec{r}_2,\omega) + \Delta\varphi_{ext}(\omega)]\end{aligned} \tag{58}$$

In the case of linear optical antenna array, the emission pattern steadily rotates from the dipole pattern of the horizontal emitter towards the dipole pattern of the vertical antenna dipole moment, when the resonant length of the antenna is reached. For nonlinear distribution of the array elements, the rotation pattern is nonlinear and depends on the assembly of the adjacent NPs. The horizontal dipole moment of the emitter plus the transverse response of the antenna and the vertical dipole moment of the antenna mode effectively determines the angular emission. As the antenna is tuned into resonance with the emission wavelength, the balance progressively shifts from the emitter dipole towards the perpendicular oriented antenna dipole, until the antenna mode dominates and fully determines the angular emission. Hence, the presence of an antenna at resonance has a major effect. It can enhance the rate with almost three orders of magnitude while the emission pattern can be fully redirected. This concept can be made use for redirecting the beam in different directions. By varying the antenna length,tuning the antenna resonance to the excitation wavelength can be done. For studying the antenna resonance patterns, monopole antennas are fabricated with different lengths. The antenna response as a function of antenna length is studied. The observed narrow molecular fluorescence spots confirm the role of the sharp tip. In principle any sharp metallic tip can confine the field through the lightening rod effect. Thus it is important to verify the role of the antenna resonance. To this end the antenna length was controllably varied between approximately 30 and 140 nm.

Optical antennas work both in excitation and emission. To enhance the excitation level, spatial localization and enhancement are used in an antenna. Let us consider the emission control of a single quantum system by the antenna. The spectral, polarization and angular response of the antenna-emitter can be studied, independent of the details of the measurement procedure and the absolute fluorescence intensity by carefully observing a single emitter. Unlike in the case of ensemble emitters, the polarization and angular emission observed are independent of how the system was illuminated, as emitter-antenna position and orientation are well defined, in a single emitter. This polarization and angular emission of a single emitter are very crucial, when it is coupled to an optical antenna. For monopole and dipole antennas, the polarization of the emission provides information about the orientation of the effective dipole moment dominating that emission which in turn determines the optical beam focusing direction. If fractal ensemble pattern is used, the fractal array concept increases the computation speed rapidly as the number of elements increase for rapid beam form computation as given in the Table 4. P refers to the

stages of growth and δ refers to the number of elements in each stage. For example for $P = 3$ and $\delta = 7$, the fractal array factor is 300 times faster to calculate than the conventional array for rapid beam forming computation.

Table 4. Illustrating the number of times faster for rapid beam forming computations.

	$P = 1$	$P = 2$	$P = 3$	$P = 4$	$P = 5$
$\delta = 3$	1	2	4	10	24
$\delta = 5$	2	6	20	78	312
$\delta = 7$	3	12	57	300	1680
$\delta = 9$	4	20	121	820	5904

The size, shape, material and enclosing medium determine the resonance of a single plasmonic nanostructure. The inter particle distance in an ensemble of NPs influences the spectral position, extinction amplitude as well as the decay dynamics (line width of the LSPR). The entire property of the array is determined by the characteristics of each particle in the array. Dense arraying or sparse arraying can be used to fulfill the requirement. A transition from near-field coupling to far field coupling, which extends to only a few tens of nanometers, takes place with increasing distance between the NPs. At the same time, there are some limitations in increasing the distance to beyond some extent. Also in the far field regime, for NPs sufficiently small compared to the operating wavelength (electrostatic limit), the NPs in the array can be seen as individual scatterers of the incoming radiation, with the scattered field being of dipolar character. However, for sufficiently large distances, the interference of the scattered field determines the optical properties of the array configuration.

6. CONCLUSION

A proper nonlinear fractal array configuration is required where no radiation is scattered into diffraction orders, for efficient receiving and focusing of optical radiation to the sub wavelength region without losing energy by scattering. By reciprocity, in order to achieve highly directive radiation into one direction, the opening of diffraction channels has to be carefully suppressed by carefully choosing the non-linearity determined by the fractal array configuration using dense or sparse array with respect to the resonant wavelength of the individual antennas in the array. The optical antenna array along with the

nonlinearities in coupled antennas and arrays concept increases the rapid beam form computation and pattern tailoring for smart beam forming using the iterated function system (IFS) concept for the nonlinear fractal optical antenna array.

ACKNOWLEDGMENT

This work was supported in part by the Canadian Government under Graduate Student Exchange Program (GSEP).

REFERENCES

1. Liberti, J. and T. S. Rappaport, *Smart Antennas for Wireless Communications: IS-95 and Third Generation CDMA Applications*, Prentice Hall, New York, 1999, ISBN-13: 978-0137192878.
2. Gianvittorio, J. P. and Y. Rahmat-Samii, "Fractal antennas: A novel antenna miniaturization technique, and applications," *IEEE Antennas and Propagation Magazine*, Vol. 44, No. 1, 20–36, Feb. 2002.
3. Best, S. R., "The fractal loop antenna: A comparison of fractal and non-fractal geometries," *IEEE Antennas and Propagation Society International Symposium*, Vol. 3, 146–149, 2001.
4. Werner, D. H. and S. Ganguly, "An overview of fractal antenna engineering research," *IEEE Antennas and Propagation Magazine*, Vol. 45, No. 1, 38–57, Feb. 2003.
5. Kim, Y. and D. L. Jaggard, "The fractal random array," *Proceedings of the IEEE*, Vol. 74, No. 9, 1278–1280, 1986.
6. Lakhtakia, A., N. S. Holter, and V. K. Varadan, "Self-similarity in diffraction by a self-similar fractal screen," *IEEE Transactions on Antennas and Propagation*, Vol. 35, No. 2, 236–239, Feb. 1987.
7. Werner, D. H., R. L. Haupt, and P. L. Werner, "Fractal antenna engineering: The theory and design of fractal antenna arrays," *IEEE Antennas and Propagation Magazine*, Vol. 41, No. 5, 37–58, Oct. 1999.
8. Liang, X., W. Zhenson, and W. Wenbing, "Synthesis of fractal patterns from concentric-ring arrays," *Electronics Letters*, Vol. 32, No. 21, 1940–1941, Oct. 1996.
9. Puente Baliarda, C. and R. Pous, "Fractal design of multiband and low side-lobe arrays," *IEEE Transactions on Antennas and Propagation*, Vol. 44, No. 5, May 1996.

10. Mandelbrot, B. B., *The Fractal Geometry of Nature*, W. H. Freeman and Company, New York, 1983, ISBN: 978-0716711865.
11. Aziz, R. S., M. A. S. Alkanhal, and A. F. Sheta, "Multiband fractal-like antennas," *Progress In Electromagnetics Research B*, Vol. 29, 339–354, 2011.
12. Romeu, J. and J. Soler, "Generalized Sierpinski fractal multiband antenna," *IEEE Transactions on Antennas and Propagation*, Vol. 49, Vol. 8, 1237–1239, 2001.
13. Levy, M., S. Bose, A. V. Dinh, and D. Sriram Kumar, "A novelistic fractal antenna for ultra wideband (UWB) applications," *Progress In Electromagnetics Research B*, Vol. 45, 369–393, 2012.
14. Karmakar, A., R. Ghatak, U. Banerjee, and D. R. Poddar, "An UWB antenna using modified Hilbert curve slot for dual band notch characteristics," *Journal of Electromagnetic Waves and Applications*, Vol. 27, No. 13, 1620–1631, 2013.
15. Dorostkar, M. A., M. T. Islam, and R. Azim, "Design of a novel super wide band circular-hexagonal fractal antenna," *Progress In Electromagnetics Research*, Vol. 139, 229–245, 2013.
16. Karmakar, A., S. Verma, M. Pal, and R. Ghatak, "Planar fractal shaped compact monopole antenna for ultra wideband imaging systems," *International Journal of Microwave and Optical Technology*, Vol. 7, No. 4, 262–267, 2012.
17. Agio, M. and A. Alù, Eds., *Optical Antennas,* Cambridge University Press, New York, 2013.
18. Gross, F. B., Ed., *Frontiers in Antennas: Next Generation Design & Engineering,* McGraw-Hill, New York, 2011.
19. Balanis, C. A., *Antenna Theory: Analysis and Design,* Harper & Row, New York; Toronto, 1982.
20. Krauss, J. D., R. J. Marhefka, and A. S. Khan, *Antennas for All Applications,* Tata McGraw-Hill, New Delhi, 2008.
21. Stutzman, W. L., *Antenna Theory and Design,* John Wiley & Sons, New York, 1998.
22. Rudge, A. W., et al. (eds.), *The Handbook of Antenna Design,* P. Peregrinus on Behalf of the Institution of Electrical Engineers, London, 1982.
23. Connor, F. R., *Antennas,* E. Arnold, London, 1989.